

SIMULATED HEAT AFFECTED ZONE IN WELDED STAINLESS STEEL 304L

Soumia Hamza¹⁾, Zakaria Boumerzoug¹⁾*, Elhadj Raouache²⁾, Fabienne Delaunois³⁾

¹⁾ Department of Mechanical Engineering, LMSM, University of Biskra, Biskra, Algeria

²⁾ Department of Civil Engineering, University of B.B.A, Algeria

³⁾ Faculté Polytechnique de Mons 56, rue de l'Epargne, B-7000 Mons, Belgique

Received: 30.05.2019

Accepted: 16.09.2019

*Corresponding author: e-mail :zboumerzoug@yahoo.fr, Tel.:+213775759694, Department of Mechanical Engineering, LMSM, University of Biskra, B.P. 145, Biskra, Algeria

Abstract

This work is a contribution study of the heat-affected zone in the real welded joint of stainless steel 304L. This zone was compared to the heat-affected zone obtained by using a thermal cycle simulation of welding. This experimental technique is based on thermal cycle simulation of welding by rapid heating and cooling treatments of the base metal in a specific simulation equipment. The samples were analyzed by scanning electron microscopy equipped with energy dispersive X-ray, and microhardness measurements. Microstructures and mechanical properties of the simulated heat affected zone were also determined. Thermal cycle simulation technique has revealed more details on the microstructure and the mechanical behavior of the heat-affected zone.

Keywords: stainless steel, thermal cycle simulation, welding, microstructures, microhardness

1 Introduction

Austenitic stainless steels are the most common and familiar types of stainless steel. They are most extremely formable and weldable [1]. Among the many 300 series austenitic stainless steel grades, AISI 304L stainless steels are extensively used in industries due to their superior low temperature toughness and high corrosion resistance [2]. Additionally, it is among the cheapest grades of stainless steels, making it the favourite choice of industry. American Iron and Steel Institute (AISI) type 304 is the formation of 300 series austenitic stainless steels is by far the oldest, largest and most important group in the stainless steel range. The L grades represent low-carbon variants with nominal carbon level of 0.03 % depending on the specification to which is manufactured, which are used for general stainless steel fabrication, elevated temperature applications and resistance to pitting corrosion [3].

It is known that the heat generated during welding induces an important temperature gradient in and around the welded area. The region outside the welded joint that is thermally affected by the welding treatment is known as the heat-affected zone (HAZ) [4]. Its property and microstructure are affected by the thermal cycle. The mechanical properties of the welded metal and the HAZ are closely related to their microstructures, which are dependent on the chemical composition of the material and the thermal history (cycles) due to the welding processes [5, 6]. The welded joints under exploitation conditions can be affected by the chemical heterogeneity or mechanical properties of base material, heat affected zone and weld metal. It has been concluded that by improving the microstructure of the HAZ, the properties of the welded joint can be improved [7]. Excessive heat input could result in a wide HAZ with low impact strength [8]. As reported

by Gu et al. [9], the degradation in strength and toughness of welded joint, is always happens in HAZ.

For this reason, weld thermal cycle simulation can be used for optimizing the welding technology since it enables some mechanical testing for properties that cannot be made on real welded joints because of small width of HAZ. Weld thermal cycle simulation facilitates gaining of results needed for optimization of high-alloy steel welding parameters, which can be further used for real-conditioned welding [10]. This technique consisted of rapid heating and cooling treatments of the base metal in specific simulation equipment. The HAZ can be simulated by heating the base metal at different temperatures, which correspond to the temperature at HAZ of the real welded joint. This technique has been used in our previous works [8, 11]. We studied the heat-affected zone by thermal cycle simulation of welded INC 738 LC alloy [11] and low carbon steel [6]. We found a similarity between the microstructure obtained by thermal cycle simulation of welding and the microstructure of the HAZ of the real welded joint.

We notice that the previous work on welding of 304L stainless steel were focused on microstructure and corrosion behavior of welded material [12-14] and there is not a specific investigation on heat affected zone of welded 304L stainless steel. The objective of this present investigation is to study the microstructures of the HAZ of 304L stainless steel by a thermal cycle simulation.

2 Experimental materials and methods

The base metal (BM) is AISI 304L Austenitic stainless steel which is used for transport gas pipeline applications, generally welded for pipeline construction. The chemical composition of 304L steel is presented in **Table 1**.

Table 1 Chemical composition of AISI 304L austenitic stainless steel (wt %)

Fe	C	Mn	Si	P	S	Ni	Cr
Balance	0.026	1.07	0.40	0.038	0.001	8.11	18.50

To obtain real welded joint, V-shaped butt welds were prepared using two consecutive passes with gas tungsten arc welding (GTAW) method and ER-308L filler was used as electrode. The chemical composition of the electrode is presented in **Table 2**. In addition, argon gas was used during welding to avoid a penetration into weld region of some undesirable elements (N₂, O₂, H₂).

Table 2 Chemical composition of the electrode (Wt.%).

Fe	C	Mn	Si	P	S	Ni	Cr
Balance	0.026	1.07	0.40	0.038	0.001	8.11	18.50

For thermal cycle simulation study, specimens 10 mm thick 10 x 57 mm² of AISI 304L Austenitic stainless steel, were heat treated for the simulator tests TCS 1405 (**Fig. 1**). Simulation studies of thermal cycles consisted of resistive heating of samples. Based on phase diagram of Fe-Cr, thermal cycles were simulated at the following temperatures: 600°C, 700°C, 800°C, 900°C, 1100°C, and 1200°C (**Fig. 2**).

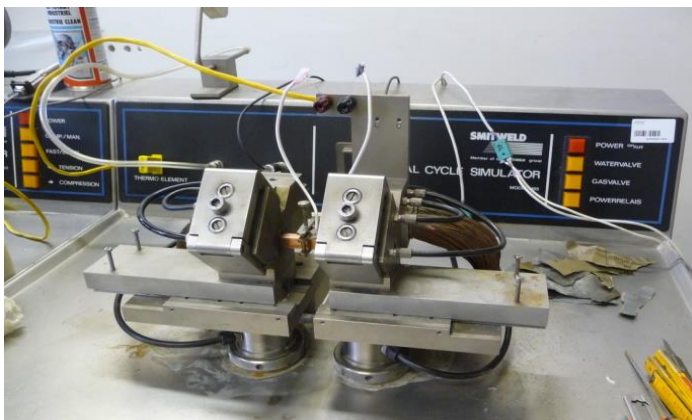
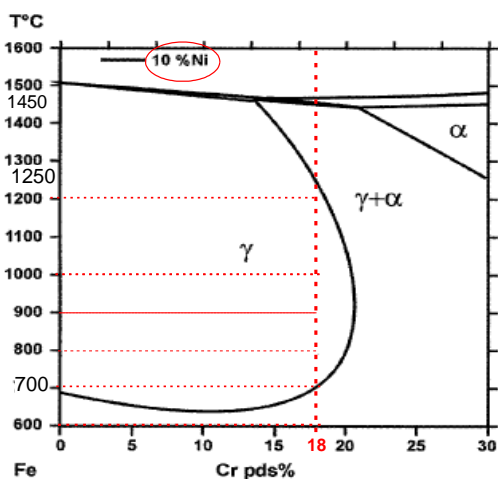
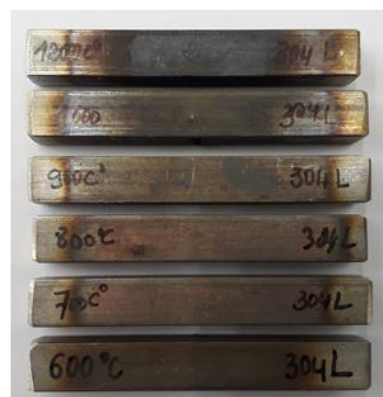


Fig. 1 Smitweld thermal cycle simulator in application



(a)



(b)

Fig. 2 (a): Equilibrium diagram of Fe-Cr [5] and (b) heated samples by thermal cycle simulator

The specimens for metallographic examination were polished using different grades of emery papers. Final polishing was done using the diamond compound (0.5 μm particle size) in the disc-polishing machine. Samples were etched with V2A reagent to reveal the microstructure. The etched samples were observed by Scanning Electron Microscopy (SEM) Bruker, which is equipped with an energy dispersive X-ray (EDS) detector for chemical composition microanalysis. Vickers's microhardness testing machine was employed for measuring the hardness of the specimens with 0.1 kg load.

3 Results and discussion

3.1 EDS analysis and microstructure of the base metal

The EDS spectrum of the AISI 304L austenitic stainless steel is presented in Fig. 3. The main alloying elements (Cr, Ni, Mn, Si) were detected.

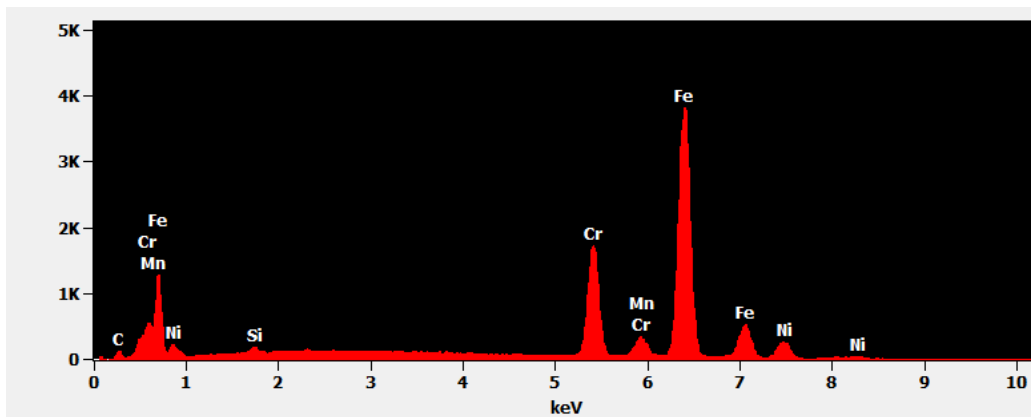


Fig. 3 EDS spectrum of AISI 304L austenitic stainless steel

The microstructure of the AISI 304L austenitic stainless steel is homogeneous and it is mainly composed of austenite phase (**Fig. 4**).

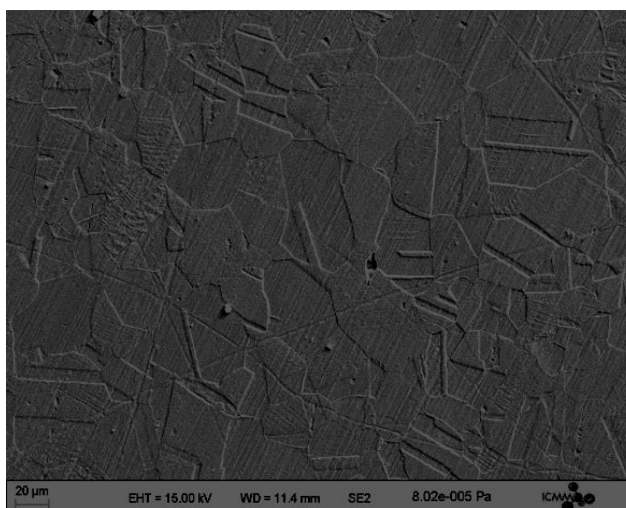


Fig. 4 Microstructure of the stainless steel 304L

3.2 Microstructure and hardness Vickers of the real welded joint

Generally, the metallurgy of the welded joint can be categorised into two major regions, the fusion zone (FZ) and the heat-affected zone (HAZ). **Fig. 5** presents the microstructure of the welded joint of the stainless steel 304L with the average hardness value of each zone. In this case, it is easy to distinguish the FZ to the rest of the zones (HAZ and BM). FZ is delimited by yellow discontinuous line. However, it is not easy to make a difference between the HAZ and BM. In addition, there is a slight difference between the hardness values between the three zones (BM, HAZ and FZ). For this reason, the investigation of HAZ by thermal cycle simulation welding is necessary.

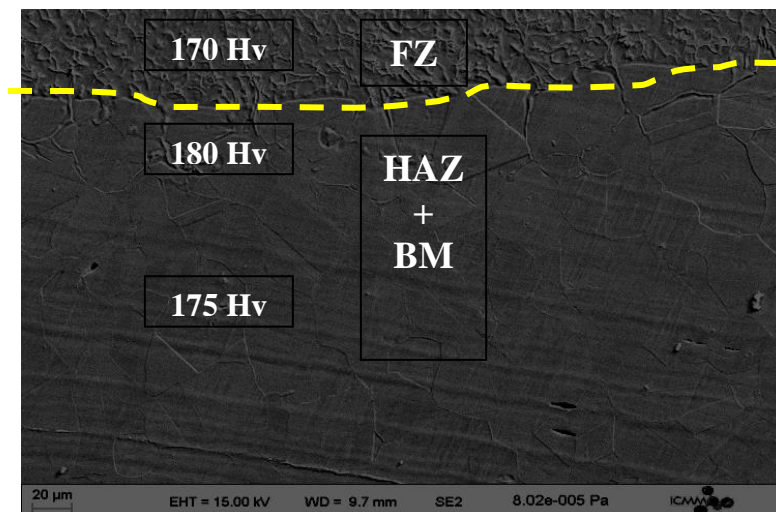


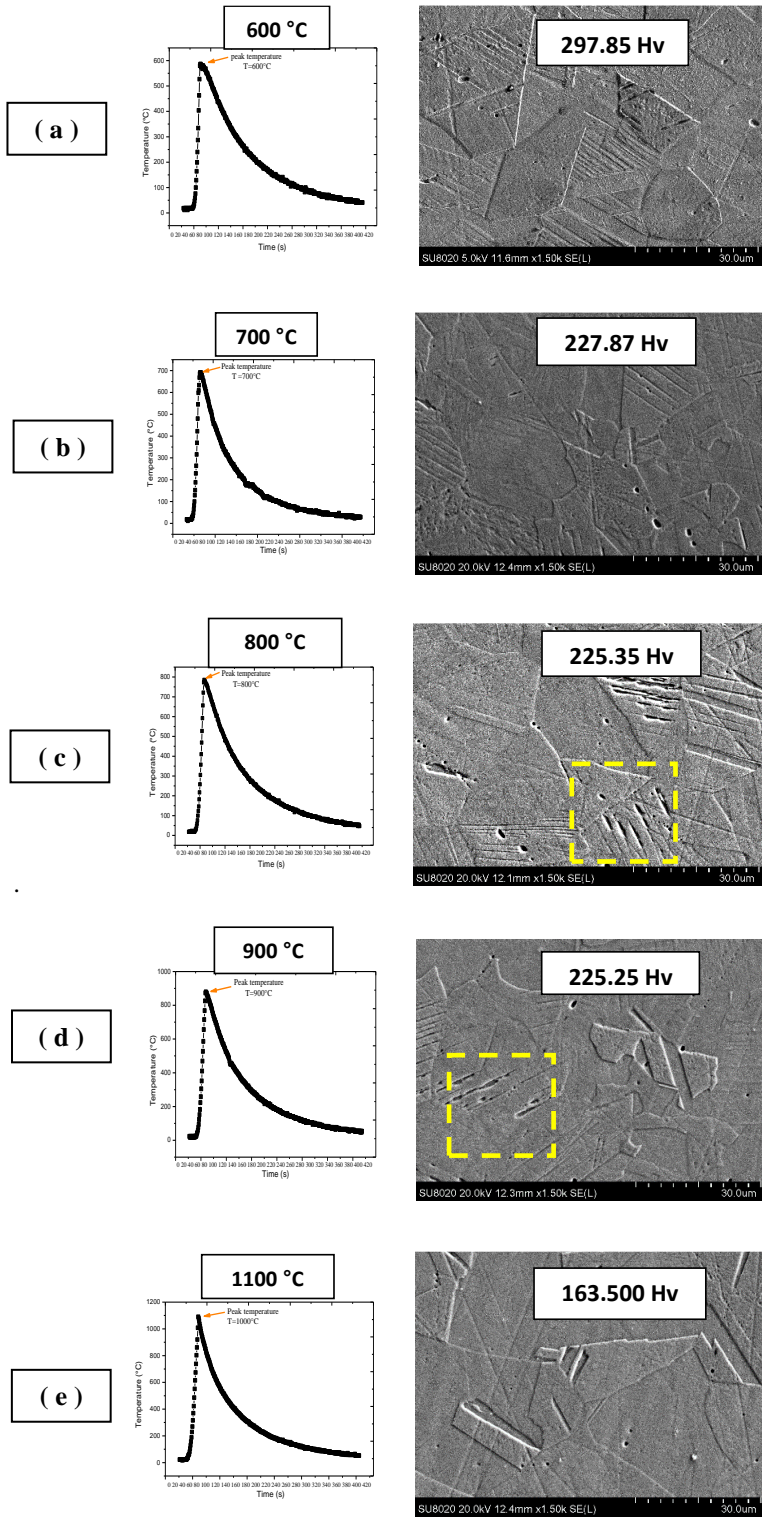
Fig. 5 Microstructure of the welded joint of stainless steel 304L

3.3 Microstructures and hardness after thermal cycles

Fig. 6 shows the microstructures of stainless steel 304L obtained after different thermal cycles (600, 700, 800, 900, 1100, and 1200 °C) with the corresponding hardness value respectively (297.85, 227.87, 225.35, 225.25, 163.500, and 162.50 Hv). The main observed transformation was the development of the grain growth reaction during the thermal cycle at 1200 °C. At this temperature, the mobility of the grain boundaries is higher as indicated by an arrow, which corresponds to the regeneration of new grains. It has been reported that austenitic steels may undergo microstructural changes in the course of the welding process or when they are exposed to elevated temperature for a shorter or longer period of time [15]. The thermal cycle at 800°C and 900 °C leads to the carbide formation as indicated by square in figure 6. The main carbides observed in 304L steel were Mn_5C_2 , Mn_7C_3 and $Mn_{23}C_6$ [16]. These hardened compound phases contribute to the increase of the hardness in HAZ.

However, with the increase of temperature more than 900 °C, the hardness HV decreases. This decrease is due to grain growth and dissolution of the carbides. It could be also attributed to a lower stress level and to change in microstructure as it has been found by Kozuh et al. [17, 18]. These authors studied the mechanical properties and microstructure of austenitic stainless steel after welding and post-weld heat treatment. In addition to this work, it has been found also that the coarse grain formation in the HAZ occurring by recrystallization and grain growth in fully austenitic metals increases susceptibility to liquation cracking, while ferrite forming composition are not susceptible [18].

Based on the above results we can deduce that the HAZ is not a homogeneous structure but it can be divided in successive subzones. The microstructure and the hardness change from the base metal to the fusion zone, i.e., the microstructure of the nearest subzone to the FZ has the lowest hardness and the highest grains size; however the nearest subzone to the BM has the highest hardness and the lowest grains size. Jelani et al. [19] concluded that the sensitivity of the mechanical properties of 304L stainless steel to temperature, i.e., the material becomes softer and more ductile with the increase of the temperature up to 900 °C. For this reason, the nearest subzone to the FZ has the lowest hardness. These hardness values are more precise than the hardness values measured on the real welded joint.



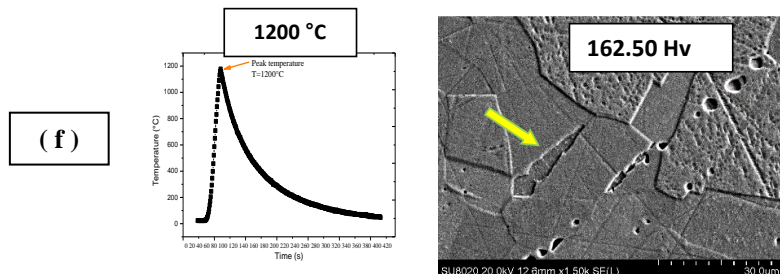


Fig. 6 Microstructures of 304L after simulation welding process and their plotted temperature-time during the welding thermal cycle (a-f)

4 Conclusion

In summary, the simulated HAZ of the welded stainless steel 304L has been investigated by the thermal cycle simulation technique and compared to the HAZ obtained from the real welded joint. The microstructural observation of the HAZ in real welded joint did not reveal more details. However, the investigation of the simulated HAZ by the thermal cycle simulation technique has given more information. The HAZ is not a homogeneous structure but it is formed with different subzones. The thermal cycle at 800 and 900 °C leads to the carbide formation. By increasing the temperature by simulation technique, the HAZ becomes softer which corresponds to the nearest subzone to the FZ. This softening phenomenon is due to the grain growth and the dissolution of carbides.

References

- [1] M. McGuire, *Stainless steel for design engineers*, ASM International, Materials Park, Ohio, 2008
- [2] W.F. Smith, *Structure and properties of engineering alloys*, 2nd ed. New York: McGraw-Hill; 1993
- [3] P. S. Korinko, S. H. Malene, *Consideration for the weldability of types 304L and 316L stainless steels*, Department of energy, U.S. 2001
- [4] A. Mostafa, S. Bordbar.: *Materials Letters*, 98, 2013, 178–181, <http://dx.doi.org/10.1016/j.matlet.2013.04.035>
- [5] Y. Chen, Y. Y. Wang, J. Gianetto: *Proceedings of the Eighteenth International Offshore and Polar Engineering Conference*, Vancouver, BC, Canada, July 6–11, 2008
- [6] Z. Boumerzoug E. Raouache Elhadj, F. Delaunois: *Materials Science and Engineering A* 530, 2011, 191–195, <http://dx.doi.org/10.1016/j.msea.2011.09.073>
- [7] K. Digheche, Z. Boumerzoug, M. Diafi : *Acta metallurgica Slovaca*, Vol. 23, No. 1, 2017, 72-78, <http://dx.doi.org/10.12776/ams.v23i1.879>
- [8] V. Gunaraj, N. Murugan: *Welding research*, 81, 2002, p. 94-98
- [9] Y. H. Guo, L. Lin, D. Zhang, L. Liu, M. K. Lei: *Metals*, Vol. 8, 2018, No. 773, p.1-14 <http://dx.doi.org/10.3390/met8100773>
- [10] M. Dunder, I. Samardžić, T. Vuherer: *Metalurgija*, Vol. 54, 2015, No. 3, p. 539-542
- [11] Z. Boumerzoug et S. Cherif : *Key Engineering Materials*, Vol. 735, 2017, p. 75-79 <http://dx.doi.org/10.4028/www.scientific.net/KEM.735.75>
- [12] G. R. Mirshekari, E. Tavakoli, M. Atapour, B. Sadeghian: *Materials and Design*, Vol. 55, 2014, p. 905–911, <http://dx.doi.org/10.1016/j.matdes.2013.10.064>

- [13] C. M. Lin, H. L. Tsai, C. D. Cheng, C. Yang: Engineering Failure Analysis, Vol. 21, 2012, p. 9–20, <http://dx.doi.org/10.1016/j.engfailanal.2011.11.014>
- [14] S. A. A. Akbari Mousavi, R. Miresmaeili: Journal of Materials Processing Technology Vol. 208, 2008, No. 1–3, No. 21, p. 383–394 <http://dx.doi.org/10.1016/j.jmatprotec.2008.01.015>
- [15] Y. Minami, H. Kimura, Y. Ihara: Mat. Sci. Tech., Vol. 2, 1986, p. 795-806, <http://dx.doi.org/10.1179/026708386790219697>
- [16] G. Maistro, PhD thesis, Low-temperature carburizing/nitriding of austenitic stainless steels, Chalmers University of Technology, Gothenburg, Sweden 2018
- [17] S. Kozuh, M. Gogic, I. Kosec: Kovove Mater. Vol. 47, 2009, p. 253-262
- [18] V. P. Kujanpaa: Met. Constr., Vol. 117, 1985, p. 40-46
- [19] M. Jelani, Z. Li, Z. Shen, N. UI Hassan, M. Sardar: Metals, Vol. 8, 2018, No. 620, p.1-13 <http://dx.doi.org/10.3390/met8080620>